# AN EFFICIENT HAZE REMOVAL ALGORITHM USING CHROMATIC PROPERTIES

*Yao Wang, Fangfa Fu*,Weizhe Xu, Jinjin Shi, Jinxiang Wang**

Harbin Institute of Technology, micro-electronic center, 2A building, YiKuang street, Harbin, China, 150086

## ABSTRACT

Fog degrades the quality of road images causing errors in stereo matching and road segmentation for Advanced Driver Assistance Systems (ADAS). Accident rates can be reduced if robust and efficient algorithms are applied for road image fog removal. Many studies have been conducted on this subject to date, but existing methods are not optimized for road images. Several daytime models cause local darkness, and blurring artifacts result in low quality haze-free images, and nighttime models are altogether inefficient.

This study focuses on dehazing daytime and nighttime images by utilizing chromatic properties to remove haze from images. The proposed method treats fog as a specular pixels of dual consistency and physical properties, and the dehazing reflection model is suitable for parallel implementation to efficiently detect fog pixels. An edge-preserving low-pass filter (a fast-bilateral filter running 230x faster than an average CPU) is used to smooth the color components' original image maximum fraction to remove noise among fog pixels. The method significantly outperforms existing baselines in regards to both efficiency and dehazing.

***Index Terms***— Dehazing, ADAS, chromatic properties, bilateral filter

## 1. INTRODUCTION

Inclement weather conditions such as fog or haze increase traffic accident rates. Large amounts of particles and water droplets in the atmosphere absorb and scatter light, causing blurring artifacts that degrade the contrast and fidelity of outdoor images. Most intelligent automatic driving systems depend on these input images to improve driver safety. These systems are substantially limited in harsh weather conditions, to this effect. Efficient and robust algorithms are in urgent demand to benefit consumer/computational photography and computer vision applications such as stereo matching [1], segmentation [2], and recognition [3].

In this study, we began by developing a dehazing reflection method to significantly enhance scene contrast and visibility; haze-free images are beneficial to the stereo matching rate. Dehazing can also provide high-quality images which aid ADAS and benefit vision algorithms such as image classification and recognition. Our primary goal is eliminating the effects of inclement weather, which is a crucial task in computer vision and pattern recognition.

## 2. RELATED WORK

Early research on this subject generally focused on haze removal from a single image based on a histogram [4]. The results of this study were conclusive, however, as single-image haze causes scattering and a threshold filter cannot accurately locate the haze. To enhance defogging performance, Schechner [5] and Shwartz et al. [6] captured images from different polarization angles to remove haze; this approach is not suitable for real-time applications, unfortunately.Deussen [7] focused on depth-mapping to remove fog via a physical model, but their approach lacks flexibility due to the proposed geometric models.

A novel haze removal method was proposed by Tan [8] utilizing local contrast image maximization via Markov Random Field (MRF) by assuming that the hazy image's local contrast is much lower than that in a haze-free image. This approach removes fog but also degrades image quality due to over-dehazing. He et al. [9] used dark channel prior (DCP) to remove haze based on the observation, however, soft matching causes this method to be computationally intensive and thus limits its application in systems.

Several approaches have been proposed to improve DCP efficiency by He et al. [9], Tarel and Hautiere [10], and Tarel et al. [11] via guided joint bilateral filtering [12–16] and guided image filtering, respectively. Kratz and Nishino [17] and Nishino et al. [18] evaluated scene radiance with a factorial Markov random filed accurately. Meng et al. [19] proposed an efficient Image dehazing method with boundary constraint and contextual regularization to restore haze-free images. Few studies have yet combined the haze removal method with road images, since most algorithms are not suitable for real time applications. Aubert et al. [20] first performed visibility enhancement via an onboard camera, but were not able to enhance object visibility. In addition, a visibility enhancement algorithm [21] dedicated to road images was proposed able to enhance background contrast. All these algorithms are incapable of producing high quality haze-free images and fast processing speeds.

In this study, we propose a novel dehazing reflection model with bilateral filter (DRBF) for image dehazing. A powerful dehazing reflection model was used to localize hazy pixels and estimate their intensity. This enabled us to estimate accurate atmospheric light and medium transmissions by changing different bilateral filter parameters. Finally, we easily removed the haze from images via the atmospheric scattering model.

## 3. DEHAZING METHOD

This section describes our dehazing method. We begin by first describing the standard atmospheric scattering model (Section 3.1). This inspires us to remove haze correctly. We then utilize dehazing reflection model via bilateral filter to secure an accurate fog pixels (Section 3.2).

### 3.1. Atmospheric Scattering Model

The following linear interpolation model proposed by McCartney [23] is widely used to describe hazy image formation:

$$I(x) = J(x)t(x) + A(1 - t(x)) \tag{1}$$

$$t(x) = \ell^{-\beta d(x)} \tag{2}$$

where $I$ represents observed color hazy image, $x$ denotes pixel position in the image coordinate, $J$ is scene radiance representing the haze-free image, $A$ represents global atmospheric light, $t$ denotes medium transmission $(0 \leq t(x) \leq 1)$, and $\beta$ and $d$ are atmosphere scattering coefficient and scene depth, respectively. The goal of haze removal is to recover $J$ from $I$. Thus, the purpose of dehazing is to estimate $A$ and $t$, then restore $J$ according to Eq. (1). The haze-free image $J(x)$ is recovered if we evaluate atmospheric light $A$ and transmission $t$ in Eq. (3).

$$J(x) = \frac{I(x) - A}{t(x)} + A \tag{3}$$

In the next section, we present our novel method via chromatic properties for estimating transmission from outdoor hazy images.

### 3.2. Dehazing reflection model

Fog and highlight features are discussed in this section. The highlight was caused by spectral energy distribution of light reflected from an object, as shown in Fig. 1(a). The appearance of this white highlight degrades image quality due to light source characteristics, thus creating a discontinuity in the diffusion area. Haze and highlight have similar feathers, including a white appearance, as shown in Fig. 1(b). This discontinuity in scene objects is a result of fog formation and highlights due to light reflection. Despite a few small differences, these can be regarded as the same problem. We then detected fog location based on dichromatic reflection model [24].

A colorful image can be denoted as a linear combination of diffuse $(I_d)$ and specular reflections $(I_s)$ as follows:

$$I(x) = I_d(x) + I_s(x) \tag{4}$$

$$I(x) = I_{haze}(x) + I_{haze-free}(x) \tag{5}$$

Inspired by dichromatic reflection model, we treated fog as specular reflections as they share similar properties. We can thus rewrite Eqs. (4) to (5) for finding foggy pixel location (specular pixels) and estimate atmospheric light value and medium transmission.

The chromaticity $\sigma_c$ can be described as:

$$\sigma_c = \frac{I_c}{\sum_{c\in\{r,g,b\}} I_c} \tag{6}$$

where $I_c$ represents colorful images with $r, g, b$ channels. We define haze-free chromaticity $\Lambda_c$ and image $I_c^D$ (dehazing image) as follows:

$$\Lambda_c = \frac{I_c^D}{\sum_{c\in\{r,g,b\}} I_c^D} \tag{7}$$

Thus, estimating maximum dehazing chromaticity $\Lambda_c$ for every pixel from a single image. We approximate $\Lambda_c$ using $\lambda_c$:

$$\sigma_{\min} = \min(\sigma_r, \sigma_g, \sigma_b) \tag{8}$$

$$\lambda_c = \frac{\sigma_c - \sigma_{\min}}{1 - 3\sigma_{\min}} \tag{9}$$

The maximum component of approximate haze-free chromaticity $\lambda$ can be computed as follows:

$$\lambda_{\max} = \max\left(\frac{\sigma_r - \sigma_{\min}}{1 - 3\sigma_{\min}}, \frac{\sigma_g - \sigma_{\min}}{1 - 3\sigma_{\min}}, \frac{\sigma_b - \sigma_{\min}}{1 - 3\sigma_{\min}}\right) \tag{10}$$

Using the approximate maximum dehazing chromaticity defined in Eq. (10), we get the haze map via:

$$I_{\text{haze}}(x) = \frac{\max_{c\in\{r,g,b\}} I_c - \lambda_{\max} \sum_{c\in\{r,g,b\}} I_c}{1 - 3\lambda_{\max}} \tag{11}$$

After evaluating maximum dehazing chromaticity in Fig. 2(a), the fog map can be obtained via Fig. 2(b). The fog map contains some black noise which causes artifact blurring and affects haze-free image quality. Black noise is indicated by red circles. We then used a bilateral filter to remove noise and refine fog map. Bilateral filter is simple and not discussed.

## 4. SCENE RADIANCE RECOVERY

### 4.1. Estimation of atmospheric light A and transmission

In this section, we describe atmospheric light estimation in more detail. Fog distribution was discovered using an accurate fog pixels in Section 3. We have chosen the top 0.1 percent brightest pixels in the map, and then selected the highest

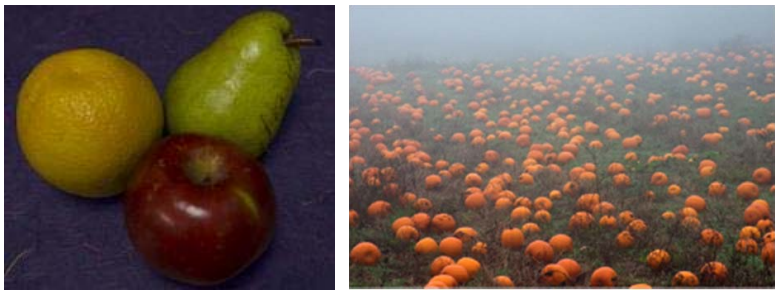

(a) (b)

**Fig. 1**. Fruit images; (a) Apple image with highlight; (b) Orange image with dense fog;

(a) (b)

**Fig. 2**. Fog map by dehazing reflection model; (a) Orange fog image; (b) Fog map with black noise;

intensity pixel in the corresponding haze image. After finding the fog map and atmospheric light A via our proposed method, we can then estimate transmission $t(x)$ so that haze-free image can be restored. We can rewrite Eq. (1) as follows:

$$t(x) = \left\| \frac{I(x) - A}{J(x) - A} \right\| = \min \left\| \frac{I(x) - A}{J(x) - A} \right\| = \frac{\min I_c(x) - A}{\min J_c(x) - A} = \frac{Ak_0 - I_{\text{haze}}(x)k_0}{Ak_0 - I_{\text{haze}}(x)k_1} \tag{12}$$

$$\begin{aligned} k_0 &= 1 - \min I_c \\ k_1 &= I_{\text{haze}} - \min I_c \end{aligned} \tag{13}$$

where $c \in \{r, g, b\}$ is color channel index, $I(x)$ is haze image, while $J(x)$ is defogged image. To evaluate $t(x)$, two coefficients $k_0$ and $k_1$ are introduced. Scene radiance is usually not as bright as atmospheric light, and thus the image looks dimmer after haze removal. By changing the values of $k_0$ and $k_1$, haze removal appears brighter than in previous methods. The values of $k_0$ and $k_1$ are established in Eq. (13), and were found to exhibit good results.

We restricted the minimum $t(x)$ value to 0.1, and thus the final representation used for haze-free image $(J(x))$ by our proposed method is:

$$J(x) = \frac{I(x) - A}{\max\{t(x, y), t_0\}} + A \tag{14}$$

## 5. EXPERIMENTAL RESULTS

We tested the effectiveness of our method on various hazy images and compared it against the methods of He [9], Meng [19], and Zhu et al. [22]. All algorithms were implemented in MatlabR2014a and hazy images were separated into two categories: Natural and synthetic. 1000 images were downloaded from kitty database in city and residential category for stereo vision. In Fig.3, we compare our approach with previous methods. The sky in Meng et al.'s result in Fig. 3(c) tends to be darker and the traffic sign of He and Zhu's method in 3(b) and 3(d) are more faint than in our results. Zhu's method employs a depth map via single image to evaluate transmission, resulting in a lack of more details after dehazing. Meng and Zhu's methods for nighttime haze images are not suitable to remove haze efficiently due to glow effect. Our method achieves better results than the others.

We evaluated the haze-free quality images via peak signal-to-noise ratio (PSNR) to achieve numerical accuracy. The PSNR is given below for He et al. [9], Meng et al. [19], and Zhu et al. [22].

PSNR results produced via different methods are shown in Table 1, where PSNR value represents image quality after dehazing. Our approach gained higher PSNR than other methods. Our approach was faster than others in large image resolution by gaining higher PSNR, as shown in Table 2. The high efficiency of our proposed method is due to the dehazing

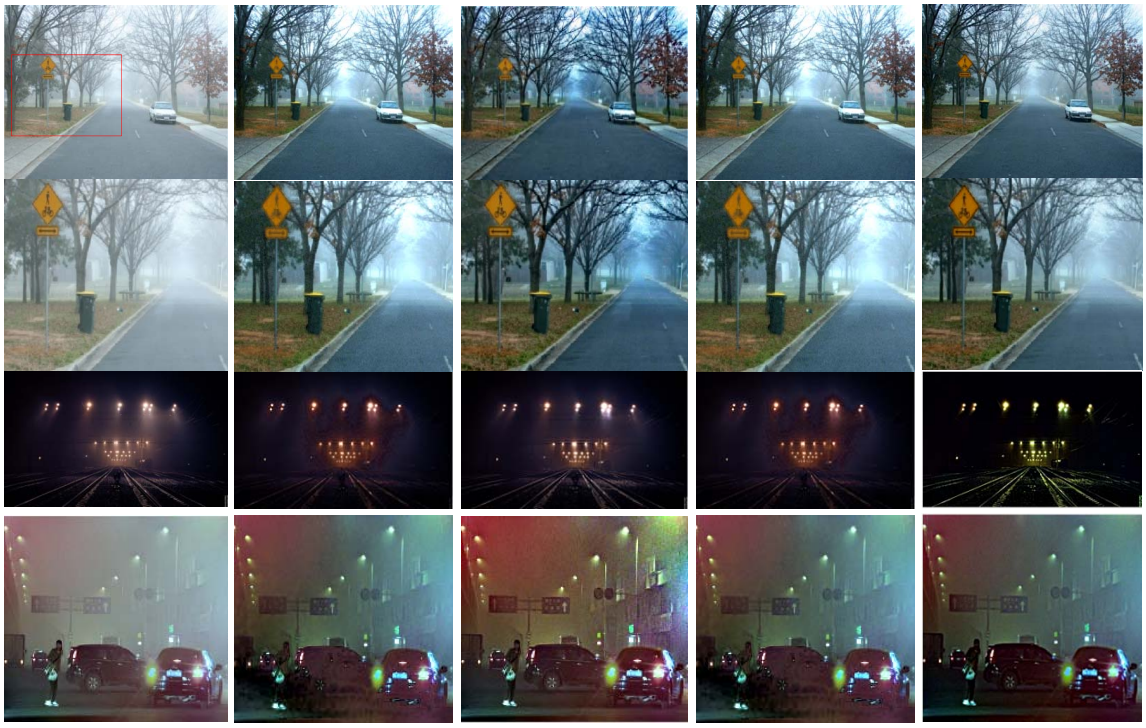

(a) (b) (c) (d) (e)

**Fig. 3**. Comparison with He et al.'s method[9],Meng et al.'s method [19] and Zhu et al.'s [22] method; From left to right: (top (a-e)) Input haze image, He et al.'s results, Meng et al.'s results, Zhu et al.'s results, and our results; (middle (a-e)) Close-up patches in the box (best viewed in color); (bottom (a-e)) Input nighttime haze road image, He et al.'s results, Meng et al.'s results, Zhu et al.'s results, and our results

reflection model via bilateral filter by significantly improving haze-free image quality and simplifying scene depth estimation and transmission.

**Table 1**. The average PSNR comparison with He et al. [9], Meng et al. [19], and Zhu et al. [22]

| Haze Image | [9] | [19] | [22] | Ours |
|---|---|---|---|---|
| magazine | 20.6 | 22.1 | 23.8 | 27.5 |
| cones | 21.5 | 22.9 | 24.3 | 29.4 |
| home | 24.2 | 25.3 | 27.1 | 32.5 |
| moebius | 23.9 | 26.6 | 28.4 | 34.6 |

## 6. CONCLUSION

In this study, we established an efficient DRBF method by observing that fog and highlight share similar physical properties. We can thus detect fog via dehazing reflection model to remove highlights. A fast bilateral filter was used to achieve an accurate fog map without black noise. Additionally, atmospheric light and medium transmission were easily estimated using our proposed method. This method is suitable for parallel implementation and the processing time is 1,024 K-B images at a video rate on an NVIDIA Geforce 8800 GTX GPU. Experimental results show that the proposed approach achieves high efficiency and outstanding dehazing effects in both daytime and nighttime conditions.

**Table 2**. Running time (seconds) of haze removal in [9],[19] and [22] with the proposed algorithm on CPU

| Haze image | [9] | [19] | [22] | Ours |
|---|---|---|---|---|
| 600*450 | 12.88 | 4.68 | 3.15 | 2.12 |
| 1024*768 | 37.85 | 15.23 | 6.78 | 5.68 |
| 1803*1080 | 93.77 | 25.66 | 14.29 | 10.10 |

## 7. ACKNOWLEDGMENTS

This work was supported by a grant from National Natural Science Foundation of China (NSFC,No. 61504032).

## 8. REFERENCES


[1] Shi J, Fu F, Wang Y, et al. Stereo Matching with Improved Radiometric Invariant Matching Cost and Disparity Refinement[C]//International Conference on Intelligent Computing. Springer International Publishing, 2016: 61-73.

[2] L. Shao, L. Liu, and X. Li, "Feature learning for image classification via multiobjective genetic programming," IEEE Trans. Neural Netw. Learn.Syst., vol. 25, no. 7, pp. 1359–1371, Jul. 2014.

[3] Y. Luo, T. Liu, D. Tao, and C. Xu, "Decomposition-based transfer distance metric learning for image classification," IEEE Trans. Image Process., vol. 23, no. 9, pp. 3789–3801, Sep. 2014.

[4] J.-Y. Kim, L.-S. Kim, and S.-H. Hwang, "An advanced contrast enhancement using partially overlapped sub-block histogram equalization," IEEE Trans. Circuits Syst. Video Technol., vol. 11, no. 4, pp. 475–484, Apr. 2001.

[5] Y. Y. Schechner, S. G. Narasimhan, and S. K. Nayar, "Instant dehazing of images using polarization," in Proc. IEEE Conf. Comput. Vis. Pattern Recognit. (CVPR), 2001, pp. I-325–I-332.

[6] S. Shwartz, E. Namer, and Y. Y. Schechner, "Blind haze separation," in Proc. IEEE Conf. Comput. Vis. Pattern Recognit. (CVPR), vol. 2. 2006, pp. 1984–1991.

[7] J. Kopf, B. Neubert, B. Chen, M. Cohen, D. Cohen-Or, O. Deussen, M. Uyttendaele, and D. Lischinski. Deep photo: model-based photograph enhancement and viewing. In ACM SIGGRAPH Asia 2008, pages 116:1–116:10, 2008.

[8] R. T. Tan, "Visibility in bad weather from a single image," in Proc. IEEE Conf. Comput. Vis. Pattern Recognit. (CVPR), Jun. 2008, pp. 1–8.

[9] K. He, J. Sun, and X. Tang, "Guided image filtering," IEEE Trans. Pattern Anal. Mach. Intell., vol. 35, no. 6, pp. 1397–1409, Jun. 2013.

[10] J.-P. Tarel and N. Hautiere, "Fast visibility restoration from a single color or gray level image," in Proc. IEEE 12th Int. Conf. Comput. Vis. (ICCV), Sep./Oct. 2009, pp. 2201–2208.

[11] J.-P. Tarel, N. Hautière, L. Caraffa, A. Cord, H. Halmaoui, and D. Gruyer, "Vision enhancement in homogeneous and heterogeneous fog," IEEE Intell. Transp. Syst. Mag., vol. 4, no. 2, pp. 6–20, Apr. 2012.

[12] C. Tomasi and R. Manduchi, "Bilateral filtering for gray and color images," in Proc. 6th Int. Conf. Comput. Vis. (ICCV), Jan. 1998, pp. 839–846.

[13] S. Paris and F. Durand, "A fast approximation of the bilateral filter using a signal processing approach," in Proc. Eur. Conf. Comput. Vis., 2006, pp. 568–580.

[14] F. Porikli, "Constant time O(1) bilateral filtering," in Proc. IEEE Conf. Comput. Vis. Pattern Recognit. (CVPR), Jun. 2008, pp. 1–8.

[15] Q. Yang, K.-H. Tan, and N. Ahuja, "Real-time O(1) bilateral filtering," in Proc. IEEE Conf. Comput. Vis. Pattern Recognit. (CVPR), Jun. 2009, pp. 557–564.

[16] A. Adams, N. Gelfand, J. Dolson, and M. Levoy, "Gaussian KD-trees for fast high-dimensional filtering," in Proc. ACM SIGGRAPH, 2009, pp. 21:1–21:12.

[17] L. Kratz and K. Nishino, "Factorizing scene albedo and depth from a single foggy image," in Proc. IEEE 12th Int. Conf. Comput. Vis. (ICCV), Sep./Oct. 2009, pp. 1701–1708.

[18] K. Nishino, L. Kratz, and S. Lombardi, "Bayesian defogging," Int. J. Comput. Vis., vol. 98, no. 3, pp. 263–278, Jul. 2012.

[19] G. F. Meng, Y. Wang, J. Duan, S. Xiang, and C. Pan, "Efficient image dehazing with boundary constraint and contextual regularization," in Proc. IEEE Int. Conf. Comput. Vis. (ICCV), Dec. 2013, pp. 617–624.

[20] N. Hautière, J.-P. Tarel, J. Lavenant, and D. Aubert. (2006). Automatic fog detection and estimation of visibility distance through use of an onboard camera. Mach. Vis. Applicat. [Online]. 17(1), pp. 8–20. Available: http://perso.lcpc.fr/tarel.jean-philippe/publis/mva06.html

[21] N. Hautière and D. Aubert, "Contrast restoration of foggy images through use of an onboard camera," in Proc. IEEE Conf. Intelligent Transportation Systems (ITSC'05), Vienna, Austria, 2005, pp. 1090–1095.

[22] Zhu Q, Mai J, Shao L. A fast single image haze removal algorithm using color attenuation prior[J]. IEEE Transactions on Image Processing, 2015, 24(11): 3522-3533.

[23] E. J. McCartney, Optics of the Atmosphere: Scattering by Molecules and Particles. New York, NY, USA: Wiley, 1976.

[24] Tan R T, Ikeuchi K. Separating reflection components of textured surfaces using a single image[J]. IEEE transactions on pattern analysis and machine intelligence, 2005, 27(2): 178-193.